

CDSM - Casual Inference using Deep Bayesian Dynamic Survival Models

Jie Zhu

*Centre for Big Data Research in Health (CBDRH)
University of New South Wales
Kensington, NSW 2052, Australia*

ELLIOTT.ZHU@UNSW.EDU.AU

Blanca Gallego

*Centre for Big Data Research in Health (CBDRH)
University of New South Wales
Kensington, NSW 2052, Australia*

B.GALLEGO@UNSW.EDU.AU

Editor: -

Abstract

Causal inference in longitudinal observational health data often requires the accurate estimation of treatment effects on time-to-event outcomes in the presence of time-varying covariates. To tackle this sequential treatment effect estimation problem, we have developed a causal dynamic survival model (CDSM) that uses the potential outcomes framework with the Bayesian recurrent sub-networks to estimate the difference in survival curves. Using simulated survival datasets, CDSM has shown good causal effect estimation performance across scenarios of sample dimension, event rate, confounding and overlapping. However, we found increasing the sample size is not effective if the original data is highly confounded or with low level of overlapping. In two large clinical cohort studies, our model identified the expected conditional average treatment effect and detected individual effect heterogeneity over time and patient subgroups. The model provides individualized absolute treatment effect estimations that could be used in recommendation systems.

Keywords: Survival Analysis; Causal Inference; Bayesian Machine Learning; Recurrent Subnetworks.

1. Introduction

While randomized experiments are the gold standard in the comparison of interventions, it has become clear that observational studies using Big Data have an important role to play in comparative effectiveness research (Gallego et al., 2013). As a result, the last few years have seen a surge of studies proposing and comparing methods that can estimate the effect of interventions from routinely collected data. In particular, new methods have emerged that can investigate the heterogeneity of treatment effect. In the health domain, these methods make use of Medical Claims (Wendling et al., 2018) and Electronic Health Record (EHR) data and have been driven by the move towards personalized care (Kravitz et al., 2004).

In spite of significant progress, there remain challenges that must be addressed. In particular, no off-the-shelf treatment effect algorithm exists that takes full consideration of the temporal nature of medical data including: patient history, time-varying confounders, time-varying treatment and time-to-event outcomes. Accounting for the temporal nature

of medical information is important when informing clinical guidelines or designing clinical decision support systems, since they underpin clinicians’ response to disease progression and patient deterioration.

As a motivating example, early detection and treatment of sepsis are critical for improving sepsis outcomes, where each hour of delayed treatment has been associated with roughly a 4-8% increase in mortality (Kumar et al., 2006). To help address this problem, clinicians have proposed new definitions for sepsis (Johnson et al., 2018), but the fundamental need to detect and treat sepsis early still remains. In this context, time-dependent confounders such as the count of white blood cells, partial pressure of oxygen (PaO_2) and fraction of inspired oxygen (FiO_2) will be affected by the previous administration of antibiotics or use of mechanical ventilation (MV). Similarly, the treatment effects in chronically ill patients (such as Atrial Fibrillation or Diabetes) changes with shifts in the patient’s risk profile and accumulates over time. The challenge of capturing the history of time-varying bio-markers and other risk factors pervades the prediction of time-to-event outcomes and the associated treatment effect in the clinical decision process.

Our aim, therefore, is to use longitudinal health record data to predict the risk of a target outcome in terms of survival probability and to estimate the corresponding survival treatment effect for individuals or patient groups. The standard approach hinges on outcome models that learn from a snapshot of baseline covariates and a static binary treatment assignment. When required, the temporality starts from the initiation of the follow-up is incorporated ‘manually’, for example by defining maximum, cumulative or average values over time.

Several recent papers have described extensions on static survival outcome models (Gensheimer and Narasimhan, 2019; Rose and van der Laan, 2011) to predict longitudinal time-to-event outcomes, including methods such as Longitudinal Targeted Maximum Likelihood Estimation (LTMLE) (Schomaker et al., 2019) and Dynamic DeepHit (Lee et al., 2020a). However, LTMLE fails to incorporate the dimensionality and complexity of EHR data while Dynamic DeepHit does not capture the causal effect from the longitudinal survival outcomes.

Conventionally, hazard ratio (HR) is used as the effect measure in causal inference with time-to-event outcomes. Despite the potential violation of constant HR assumption in the Cox model, it is hard to interpret HRs due to selection bias as the susceptible individuals used to calculate HR are depleted under different rate between the treatment and control groups. As an alternative, in this study we estimate the absolute treatment effect in terms of the difference in the potential survival curves under treatment or control conditions at the individual level (Zhu and Gallego, 2020a).

In order to estimate the absolute treatment effect, potential survival probabilities in the control and treatment groups are modeled using a novel deep-learning dynamic estimation of time-to-event (survival) outcomes. The difference in individual potential survival curves under treatment and control conditions is carried out given observed past history and treatment assignment. We call this model Causal Dynamic Survival Model (CDSM).

The key characteristics of the proposed algorithm are: 1) it learns from the pattern of observed and missing covariates in longitudinal data; 2) it captures treatment specific risks by employing potential-outcome sub-networks for treatment and control conditions; and 3) it quantifies the uncertainty of the model estimations with Bayesian dense layers.

An outline of this paper is as follows. Section 2 describes the methodology to estimate the longitudinal survival outcomes and treatment effect. In Section 3, we introduce a set of simulation studies, case studies and model evaluation techniques. Sections 4 provides the results. We end with a discussion.

2. Methods

2.1 Related works

We focus on methods for estimating survival outcomes and treatment effects over time with time-varying covariates.

The standard method such as the landmark analysis (Houwelingen, 2007) uses the Cox model (David, 1972) to estimate the treatment effect with time-varying covariates. In the landmark analysis, the instantaneous probability of experiencing an event at time t given covariates $X(t)$ is defined as a hazard function: $h(t|X(t)) = h_0 \exp(\beta'X(t))$, where β is a vector of constants, and h_0 is the baseline risk of having an event at time 0. When censoring is not considered, a Cox model compares the risk of an event between treatment and control conditions at each time t regardless of previous history of $X(t)$ or history of treatment conditions. The piecewise constant Cox model (Recknor and Gross, 1994) extends the constant β to $\beta(t)$ thus allowing for time-varying effect. However, neither model takes into account the longitudinal history of covariates and both treat missing covariates either by imputing their value or removing the incomplete observations.

To address these limitations, joint models were proposed to jointly describe both longitudinal and survival processes (Henderson, 2000; Ibrahim et al., 2010). In particular, a joint model comprises two sub-models: one for repeated measurements of time-varying covariates and the other for the time-to-event data such as a Cox model. They are linked by a function of shared random effects. To find a full representation of the joint distribution of the two models, model needs to be correctly specified for both processes. Thus, model mis-specification and computation effort significantly limit the estimation accuracy of this approach when applied to high-dimensional EHR data.

Recently, data-driven models such as recurrent neural networks (Bica et al., 2020; Lee et al., 2020a) have been proposed to learn efficiently from EHR data with complex longitudinal dependencies. For example, Dynamic DeepHit (Lee et al., 2020a) is a longitudinal outcome model which learns the joint distribution of survival times and competing events from a sequence of longitudinal measurements with a recurrent neural network structure. As a single outcome prediction model, DeepHit does not provide the explanatory mechanism for causal inference.

On the other hand, the Counterfactual Recurrent Network (CRN) (Bica et al., 2020) estimates the average longitudinal treatment effect on continuous outcomes by correcting for time-varying confounding using domain adversarial training (DAT). However, the efficacy of DAT depends on the feature alignment in source (control) and target (intervention) domains (Blitzer et al., 2006), that is, whether the covariates observed under treatment and control conditions have similar distributions (i.e., overlapping). As shown in the original work, the DAT is sensitive to the overlapping among covariates, and drops in estimation performance with the level of overlapping like other existing causal inference algorithms such as the TMLE (Rose and van der Laan, 2011) and Causal Forest (Athey et al., 2019).

There is a lack of studies dedicated to estimate the survival casual effect from longitudinal EHR data. We fill in this gap by extending our previous work on modeling treatment effect on time-to-event outcomes from static covariates (Zhu and Gallego, 2020b) to time-varying (longitudinal) covariates. We choose a Bayesian recurrent neural network as the outcome model. Neural networks learn more efficiently from trajectories of covariates than semi-parametric or parametric methods such as Super-learner and Cox models, while the Bayesian layers capture the uncertainty of network estimations. Both the baseline survival probability and its interaction with treatment can vary with time free from the proportional hazard assumption.

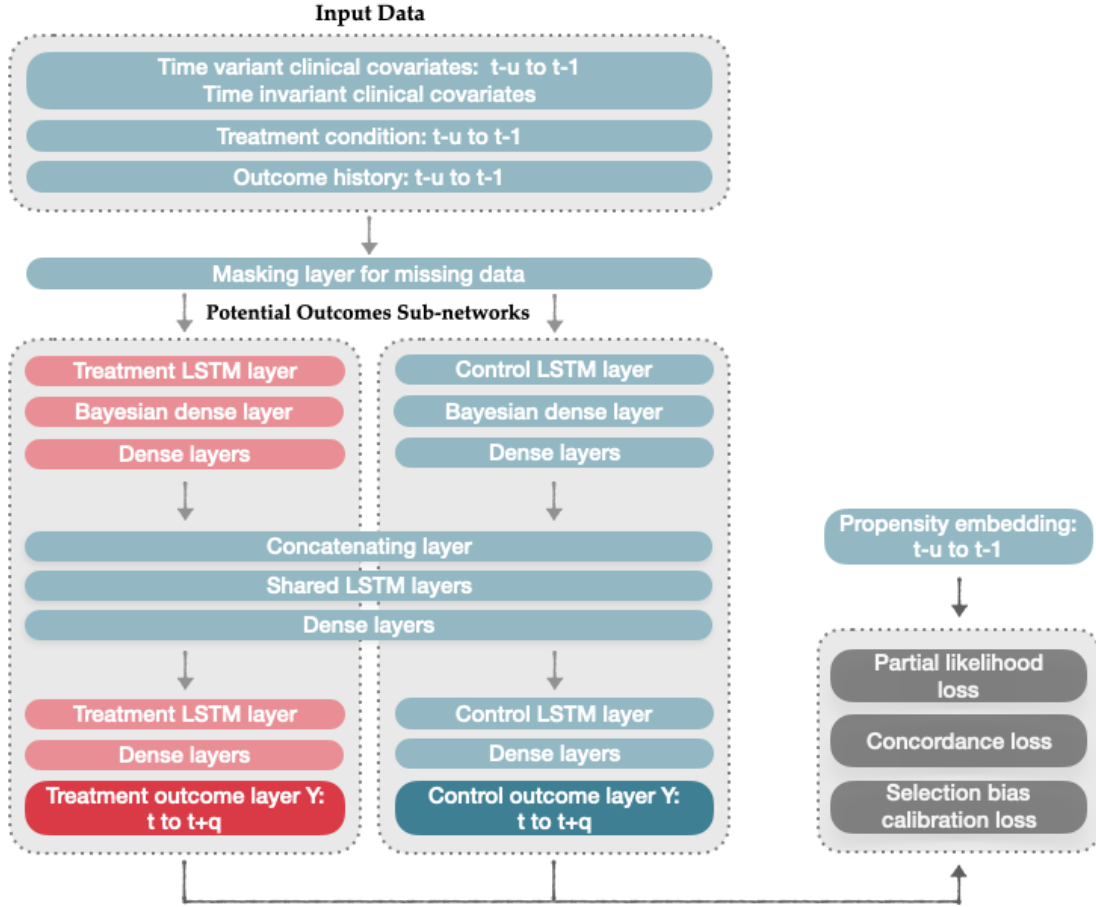


Figure 1: Illustration of the causal dynamic survival model (CDSM) Abbreviations: t , the prediction time; $t+q$, the lead time (where q is the length of forecasting window); $t-u$, the memory (where u is the length of history window)

In lieu of a single outcome model (like DeepHit) for estimating the joint distribution of the observed failure/censor times, CDSM (see Figure 1) first captures the information from treated and control observations separately, and then it encodes the information with a shared sub-network. The encoded information is fed into counterfactual sub-networks to predict the expected survival outcomes given either treatment or control conditions. The

dedicated sub-networks explicitly model the risks originated from patient baseline covariates and their interaction between treatment conditions.

Finally, we adjust for bias in the counterfactual outcomes arising from non-random treatment allocation in observational studies. The difference between the counterfactual outcomes will give us the calibrated estimate of treatment effects. In the rest of this section, we formally define the research problem and explain the construction of CDSM.

2.2 Definition of longitudinal survival treatment effect

To formalize the framework for causal inference for longitudinal survival outcomes, we follow the notations in previous studies (Imai and Strauss, 2011; Zhu and Gallego, 2020b). Suppose we observe a sample \mathcal{O} of n independent observations generated from an unknown distribution \mathcal{P}_0 :

$$\mathcal{O} := (X_i(t), Y_i(t), A_i(t), t_i = \min(t_{s,i}, t_{c,i})), i = 1, 2, \dots, n$$

where $X_i(t) = (X_{i,1}(t), X_{i,2}(t), \dots, X_{i,d}(t))$, $d = 1, 2, \dots, D$ are baseline covariates at time t , $t = 1, 2, \dots, \Theta$, with Θ being the maximum follow-up time of the study; $A(t)_i$ is the treatment condition at time t , $A(t)_i = 1$ if observation i receives the treatment and $A(t)_i = 0$ if it is under control condition; $Y_i(t)$ denotes the outcome at time t , $Y_i = 1$ if i experienced an event and $Y_i = 0$ otherwise; t_i is determined by the event or censor time, $t_{s,i}$ or $t_{c,i}$, whichever happened first.

For each individual i , we define the hazard rate $h(t)$, the probability of experiencing an event in interval $(t - 1, t]$, as:

$$h(t) := \Pr(Y(t) = 1 \mid \bar{A}(t, u), \bar{X}(t, u)), \quad (1)$$

where \bar{A} and \bar{X} are the history of treatments and covariates from $t - u$ to $t - 1$ with u being the length of the observation history. Thus, the probability that an uncensored individual will experience the event in time t can be written as a product of terms, one per period, describing the conditional probabilities that the event did not occur since time 0 to $t - 1$ but occur in period $(t - 1, t]$:

$$\begin{aligned} \Pr(t_{s,i} = t) &= h(t)(1 - h(t - 1))(1 - h(t - 2)) \cdots (1 - h(0)) \\ &= h(t) \prod_{j=0}^{t-1} (1 - h(j)). \end{aligned}$$

similarly, the probability that a censored individual will experience an event after time t can be written as a product of terms describing the conditional probabilities that the event did not occur in any observations:

$$\begin{aligned} S(t) &= \Pr(t_{s,i} > t) \\ &= (1 - h(t))(1 - h(t - 1))(1 - h(t - 2)) \cdots (1 - h(0)) \\ &= \prod_{j=0}^t (1 - h(j)). \end{aligned} \quad (2)$$

which is the population survival function.

Following Rosenbaum and Rubin's potential outcomes framework (Rosenbaum and Ruban, 1983), we assume the data is not confounded if: 1) the history of treatment assignment \bar{A} is independent of the survival outcome S given the history \bar{X} and 2) the censoring is non-informative conditioned on the treatment assignment (coarsening at random). Under these assumptions, the conditional average treatment effect (CATE) of i can be defined as:

$$\begin{aligned} \Psi(\bar{X}, t) = & \mathbb{E}_{\bar{X}=\bar{x}(t,u)} [\mathbb{E}[S(t)|\bar{A}(t,u) = 1, \bar{X} = \bar{x}(t,u)] - \\ & \mathbb{E}[S(t)|\bar{A}(t,u) = 0, \bar{X} = \bar{x}(t,u)]] \end{aligned} \quad (3)$$

where $\bar{A}(t,u) = 1$ means the patient would be under the treatment from $t-u$ to t and $\bar{A}(t,u) = 0$ means the patient would be under control for the same period. Similarly, we define the individual treatment effect (ITE) as:

$$\psi(\bar{X}, t) = \mathbb{E}[S(t)|\bar{A}(t,u) = 1, \bar{X} = \bar{x}(t,u)] - \mathbb{E}[S(t)|\bar{A}(t,u) = 0, \bar{X} = \bar{x}(t,u)] \quad (4)$$

We built a Bayesian recurrent neural network, CDSM, that can estimate the quantities specified in Equations (2), (3) and (4). To quantify the selection bias over time, we first define the potential outcomes $Y_1 = \mathbb{E}[S(t)|\bar{A}(t,u) = 1, \bar{X} = \bar{x}(t,u)]$ and $Y_0 = \mathbb{E}[S(t)|\bar{A}(t,u) = 0, \bar{X} = \bar{x}(t,u)]$, and then decompose Equation (3) into:

$$\begin{aligned} \Psi(\bar{X}, t) = & \mathbb{E}_{\bar{X}=\bar{x}(t,u)} [\mathbb{E}[Y_1 - Y_0|\bar{A}(t,u) = 1] + \\ & \mathbb{E}[Y_0|\bar{A}(t,u) = 1] - \mathbb{E}[Y_0|\bar{A}(t,u) = 0]], \end{aligned} \quad (5)$$

where the first term of the equation is the average treatment effect on treated (ATT) and the sum of the second and third term is the selection bias. CDSM contains a counterfactual sub-network to model the potential distributions of Y_1 and Y_0 and a shared network to learn the joint distribution of all observations. Its loss function is designed to minimize the selection bias in Equation (5).

The target outcome $Y^M(t)$ for the model training is defined similar to a multivariate logistic regression but with an additional term $C(t)$ to capture the censoring:

$$\begin{aligned} Y_i^M = & \begin{bmatrix} 0_1, 0_2, \dots, 0_{t_i-1}, 1_{t_i}, 1_{t_i+1}, \dots, 1_\Theta \\ C_i \end{bmatrix}, \text{ where} \\ C_i = & \begin{cases} (0_1, 0_2, \dots, 0_{t_i-1}, 1_{t_i}, 0_{t_i+1}, \dots, 0_\Theta), & \text{if event occurred} \\ (0_1, 0_2, \dots, 0_\Theta), & \text{if censored} \end{cases} \end{aligned} \quad (6)$$

The output of our model will be a sequence of predicted probabilities corresponding to the first row of Y_i^M and is interpreted as the estimated hazard rate in each time period, $\hat{h}(j)$.

Then the estimated survival curve will be given by $\hat{Y}(t) = \prod_{j=0}^t (1 - \hat{h}(j))$. CDSM estimates the potential outcomes, \hat{Y}_1 and \hat{Y}_0 , when the patient receives the control/comparator intervention during the history windows. The difference, $\hat{Y}_1 - \hat{Y}_0$, estimates the individual treatment effect defined in Equation (4).

To compare the absolute measure of treatment effect with the conventionally reported hazard ratio, we define an empirical hazard ratio as:

$$HR^*(t) = \frac{1}{n} \sum_i \frac{\hat{h}(t \mid \bar{A}(t, u)_i = 0, \bar{X} = \bar{x}(t, u)_i)}{\hat{h}(t \mid \bar{A}(t, u)_i = 1, \bar{X} = \bar{x}(t, u)_i)} \quad (7)$$

where n is the number of observations in a sample.

2.3 Building the model

Our proposed model estimates the longitudinal counterfactual survival outcomes and the difference between the two counterfactual outcomes is the estimated individual treatment effect (ITE). The model is illustrated in Figure 1 and contains:

- A masking layer taking account of informative missingness in longitudinal data (Che et al., 2018), which consists of two representations of missing patterns, i.e., a masking vector $M_t \in \{0, 1\}^D$ to denote which variables are missing at time t , and a real vector $\delta_t \in \mathbb{R}^{D, \Theta}$ to capture the time interval for each variable d since its last observation over Θ time points. The masking layer takes as inputs the matrix $(\bar{X}(t-1), \bar{Y}(t-1), \bar{A}(t-1))$ and produces as output a matrix $(\bar{M}(t-1), \bar{\delta}(t-1), \bar{X}(t-1), \bar{Y}(t-1), \bar{A}(t-1))$, where the overlines indicate the corresponding vector observed during the history window, $[t-u, t-1]$, t is the prediction time and u is the length of history window. This layer effectively uses the missing data patterns to achieve better predictions;
- Counterfactual recurrent sub-networks with Long Short-Term Memory (Hochreiter and Schmidhuber, 1997) (LSTM) units capturing the relationship between the treatment-specific risk and the longitudinal measurement. The treatment-sub-network takes as inputs the matrix $(\bar{M}(t-1), \bar{\delta}(t-1), \bar{X}(t-1), \bar{Y}(t-1), \bar{A}(t-1))$ with observations masked at $A(t-1) = 0$, and the control-sub-network masked at $A(t-1) = 1$;
- Bayesian dense layers with Flipout estimator (Wen et al., 2018) capturing the uncertainty of the network, the prior of the layer weights is set to the standard normal distribution;
- A shared recurrent sub-network with densely connected layers mapping the outcomes of each counterfactual sub-network into one output vector;
- Potential outcomes LSTM and dense layers making predictions of step-ahead time-varying covariates and log odds of the binary outcomes at each time interval given and $(\bar{X}(t-1), \bar{Y}(t-1), \bar{A}(t-1) = 0)$; and
- Counterfactual outcome layers converting log odds into the conditional probability of surviving the intervals within the prediction window, $[t, t+q]$, where q is the length of the window.

The counterfactual conditional probability of failure or censoring is plugged into the model's loss function.

2.4 Training the model

To train our neural network, we vectorized each individual event/censoring time to construct the target outcome in Equation (6) and apply a loss function with three components:

1) the partial log likelihood loss of the joint distribution of the first failure time and the corresponding event or censoring over time:

$$\begin{aligned}\mathcal{L}_1 &= \sum_t \ln \left(\prod_{i=1}^n \left[\hat{h}_i(t) \prod_{j=0}^{t-1} (1 - \hat{h}_i(j)) \right]^{1-c_i} \left[\prod_{j=0}^t (1 - \hat{h}_i(j)) \right]^{c_i} \right) \\ &= \sum_t \sum_{i=1}^n \left[(1 - c_i) \ln \left(\frac{\hat{h}_i(t)}{1 - \hat{h}_i(t)} \right) + \sum_{j=0}^t \ln(1 - \hat{h}_i(j)) \right]\end{aligned}$$

2) the rank loss function to capture the concept of concordance in survival analysis (Frank et al., 1982): a subject who experienced an event at time t should have a higher probability of failure than a subject who censored. We count the number of acceptable pairs of estimated hazard rate $\{\hat{h}_i(t), \hat{h}_j(t)\}$ in the loss function:

$$\mathcal{L}_2 = \sum_t \sum_{i \neq j} I_{ij}$$

where I_{ij} is an indicator function:

$$I_{ij} = 1, \text{ if } Y_i(t) = 1, Y_j(t) = 0 \text{ and } \hat{h}_i(t) > \hat{h}_j(t),$$

$I_{ij} = 0$, otherwise.

3) the calibration loss function to minimize the selection bias in Equation (5):

$$\mathcal{L}_3 = \sum_t \left(\sum_i (\hat{h}_{i,0}^*(t) | \bar{A}_i(t) = 1) - \sum_i (\hat{h}_{i,0}^*(t) | \bar{A}_i(t) = 0) \right)^2,$$

where $\hat{h}_{i,0}^*$ is the propensity adjusted potential hazard rate of i given control condition at time t using centered propensity score (Chernozhukov et al., 2018):

$$\hat{h}_i^*(t) = \frac{\hat{h}_i(t) \cdot \hat{\delta}_i(t)}{\frac{1}{n} \sum_i \hat{\delta}_i(t) \cdot \hat{P}_i(t)}$$

where $\hat{P}_i(t)$ is the estimated propensity score of receiving treatment at time t and $\hat{\delta}_i = A_i - \hat{P}_i(t)$ is the residual of the estimated propensity score. We estimate the binary propensity at each time step with a plain LSTM network with Sigmoid activation for the output and make it a pre-trained embedding (see Figure 1). The final loss function is defined as:

$$\mathcal{L} = \alpha \mathcal{L}_1 + \beta \mathcal{L}_2 + \gamma \mathcal{L}_3 \quad (8)$$

where grid search is used to locate the best weighting hyper-parameters α, β and γ .

3. Study design and databases

3.1 Simulation design

To explore the finite-sample performance of CDSM, we ran several experiments with biologically plausible longitudinal data following a previous study (Crowther and Lambert, 2013). Specially we use:

- $D - 1$ continuous covariates $X(0)_1, X(0)_2, \dots, X(0)_D \sim N(0, V)$ at time 0, where V is variance of the normal distribution and $D = \text{dis}$ the feature dimension. We update their value at time t as $X(t)_d = X(t-1)_d / \exp(-t^{0.5}) \log(t) + t^{0.5} + 0.013t^{1.5})$ to construct the time-varying baseline. This specific function of the $X(t)$ was chosen to resemble the observed covariate trajectory in the Germany breast cancer random trial (Sauerbrei et al., 2000) used in the previous study (Crowther and Lambert, 2013);
- $D - 1$ time invariant binary covariates $X_{D+1}, X_{D+2}, \dots, X_{2D} \sim \text{Binom}(0.5)$;
- A binary exposure determined at time 0: $A \sim \text{Binom}(\eta \cdot I(\sum_{d=1}^3 X(0)_d > \frac{1}{3} \sum_{d=1}^3 X(0)_d) + 0.5 \cdot (1 - \eta))$, where I is an indicator function and η controls the level of overlapping. When $\eta = 0$, the probability of receiving the treatment is 50% regardless of $X(0)$; when $\eta = 1$, the allocation follows the indicator function so that the outcome will be confounded by the first 3 continuous covariates of $X(0)$; and when $\eta = 0.5$, the chance of receiving the treatment is partially dependent on the indicator function which is $(0.5 \cdot I + 0.25)100\%$.
- Hazard rate: $h_i(t) = \frac{\log(t)}{\lambda} (0.1A_i + \beta \sum_{i=1}^D X(t)_i + 0.15 \sum_{i=D+1}^{2D} X(t)_i)$ where controls the level of confounding and λ is the scaling parameter to control the event rate R , which can be calculated using the survival outcome Y defined below;
- Survival probability $S_i(t) = \exp(-h_i(t))$;
- Censoring probability $SC_i(t) = \exp(-\frac{\log(t)}{\lambda})$, where $\lambda = 30$;
- An event indicator generated using *root-finding* (Crowther and Lambert, 2013) method at each time t : $E_i(t) = I(S_i(t) < U \sim \text{Uniform}(0, 1))$, with the event time defined by $T_i = t$ if $E_i(t) = 1$, otherwise $T_i = \max(T)$;
- A censoring indicator generated using the *root-finding* technique: $CE_i(t) = I(SC_i(t) < U \sim \text{Uniform}(0, 1))$, with the censoring time defined by $C_i = t$ if $CE_i(t) = 1$, otherwise $C_i = \max(T)$; and
- Survival outcome given by indicator function: $Y = I(T \leq C)$.; and the event rate is calculated as $R = \sum_{i=0}^N I(Y_i = 1)/N$, where N is the sample size. We set the value of R by grid-searching of the scaling parameter λ .

A series of experiments were conducted by changing the following parameters: $V \in \{0.1, 0.25, 0.5\}$, $D \in \{6, 12, 36\}$, $\eta \in \{0, 0.5, 1\}$, $\beta \in \{0.5, 1, 3\}$, $N \in \{1000, 2500, 5000\}$ and $R \in \{0.3, 0.1, 0.01\}$. We define our default data generation model with $V = 0.1$, $D = 6$, $\eta = 0.5$, $\beta = 1$, $N = 1000$ and $R = 0.3$. For each scenario, we generate a training sample and a testing sample using the same parameters but different random seed. All evaluations are based on the testing samples.

3.2 Case studies

We built and then applied our model to two clinical causal inference questions:

1. Effect of mechanical ventilation (MV) on in-hospital mortality for sepsis patients in the ICU. The data source for this case study is MIMIC-III, an open-access, anonymised database of 61,532 admissions from 2001–2012 in six ICUs at a Boston teaching hospital (Johnson et al., 2016). A sepsis event is defined as a suspected infection (prescription of antibiotics and sampling of bodily fluids for microbiological culture) combined with evidence of organ dysfunction, defined by a two-points deterioration of the SOFA score (Seymour, 2016). We follow previous papers (Komorowski et al., 2018; Reyna et al., 2019) for data extraction and processing. We define the treatment as the use of mechanical ventilation(MV), where previous literature has found a positive impact on patients’ in-hospital mortality.
2. Comparative effectiveness of Vitamin K Antagonists (VKAs) and Non-Vitamin K antagonist oral anticoagulants (NOAC) in preventing three combined outcomes (ischemic event, major bleeding and death) for patients with non-valvular atrial fibrillation (AF). The data source for this case study is Clinical Practice Research Datalink (CPRD) (Herrett et al., 2015) dataset. A detailed description of this cohort can be found in [refer to our AF paper - we will archive it and refer to the archived version].

A summary of the clinical cohorts is presented in Table 1. We only consider the first 20 time stamps for each patient in each dataset (i.e., the first 20 2-hour intervals for MIMIC-III, and the first 20 three-months intervals for the AF dataset.). We train the model using the 10-fold cross validation with 70% of the original data injected in each training epoch. We predict the average treatment effect estimations at each time step using the whole sample.

Table 1: Summary of case study databases

	MIMIC-III	AF
Unique patient ids	20,938	18,102
Number of event patients	2,880	3,206
Rows for the first 20 time stamp	278,504	150,193
Static features	5	49
Dynamic features	39	4

3.3 Model evaluation

The explanatory performance of CDSM is assessed with simulation studies using the four metrics described below:

Root-mean-square error (RMSE): Refers to the expected mean-squared error of the estimated individual treatment effect:

$$\text{RMSE}(t) = \frac{1}{n_k} \sum_{i_k} (\hat{\psi}_{i_k}(t) - \psi_{i_k}(t))^2$$

where n_k is the number of individuals in subgroup k and i_k is the individual indicator in each group. When estimating the ATE, we will have $n_k = N$, the sample size.

Absolute percentage bias (Bias): Defined as the absolute percentage bias in the estimated conditional average treatment effect:

$$\text{Bias}(t) = \frac{1}{n_k} \sum_{i_k} \left| \frac{\hat{\psi}_{i_k}(t) - \psi_{i_k}(t)}{\psi_{i_k}(t)} \right|$$

Coverage ratio: Refers to the percentage of times that the true treatment effect lies within the 95% quantile interval of the posterior distribution of the estimated individual treatment effect.

$$\text{Coverage}(t) = \frac{1}{n_k} \sum_{i_k} I(|\hat{\psi}_{i_k}(t) - \psi_{i_k}(t)| < CI_{i_k}(t))$$

where I is an indicator function, $I = 1$ if $I(\cdot)$ is true and 0 otherwise. CI is the 95% quantile interval of the estimations.

C-Index and AUROC: We evaluate models' discrimination performance on of the estimated survival curves with Harrell's C-index (Frank et al., 1982) and the area under the receiver operating characteristic curve (AUROC).

To test the performance of CDSM on the estimation of conditional average treatment effect (CATE) over time and subgroup sizes. We create subgroups composed of M ($M \in \{1, 5, 10, 25, 50, N\}$) randomly drawn individuals without replacement from a sample of size N . For each subgroup simulation, we drew N/M sub-samples of size M , and conducted treatment effect estimations using CDSM on each of the N/M sub-samples. We repeated and averaged the results from 50 iterations of each subgroup simulation.

3.3.1 BENCHMARK ALGORITHMS

CDSM was benchmarked against four other machine learning algorithms:

- Unadjusted CDSM (CDSM(na)): same as CDSM but set $\gamma = 0$ in the loss function of Equation (8) so that there is no correction for selection bias.
- Plain recurrent neural network with survival outcomes (RNN): remove the potential outcomes neural network in Figure 1 and set $\beta = \gamma = 0$ in Equation (8).
- Plain recurrent neural network with binary outcomes (Binary): direct prediction on the longitudinal outcome defined by the first part of Equation (6) using mean squared error as the loss function.

In order to test the effectiveness of the calibration loss function for correcting the selection bias in CDSM, we applied the inverse probability weighting (IPW) and the iterative targeted maximum likelihood estimation (TMLE) to the raw estimations from each algorithm (please refer to appendix A for a detailed explanation). We developed CDSM using Python 3.8.0 with Tensorflow 2.3.0 and Tensorflow-Probability 0.11.0 (Abadi et al., 2015) (code available at <https://github.com/EliotZhu/CDSM>).

Table 2: Estimation performance by benchmark algorithms under the default scenario

	Metrics	Algorithms			
		Binary	CDSM	CDSM(na)	RNN
Probability	AUROC	0.961	0.692	0.652	0.854
	Concordance	0.764	0.699	0.719	0.725
ATE Bias	SC (Raw)	130.1%	30.8%	35.5%	46.9%
	SC (Raw Std)	88.2%	14.4%	18.9%	14.3%
	SC (IPW)	67.8%	74.0%	69.8%	59.9%
	SC (TMLE)	40.5%	29.9%	33.8%	31.5%
	HR (Raw)	20.2%	1.0%	1.2%	6.2%
	HR (Raw Std)	16.3%	0.9%	1.0%	3.9%
	HR (IPW)	68.6%	40.0%	39.9%	46.1%
	HR (TMLE)	30.8%	10.6%	15.1%	11.2%
ITE RMSE	Survival Curve (Raw)	0.191	0.050	0.058	0.103
	HR (Raw)	0.715	0.010	0.022	0.249

All metrics are averaged across 50 independent simulations over 30 time points from the test dataset under the default scenario.

Abbreviations: *SC (Raw)*: the raw estimation of the average treatment effect (ATE) or the individual treatment effect (ITE) measured by the difference in survival curves under control and treatment conditions. *HR (Raw)*: the raw ATE or ITE estimations specified in Equation (7). *IPW*: the inverse probability weighting adjustment to the raw estimation of ATE. *TMLE*: the iterative targeted maximum likelihood estimation adjustment to the raw ATE.

4. Results

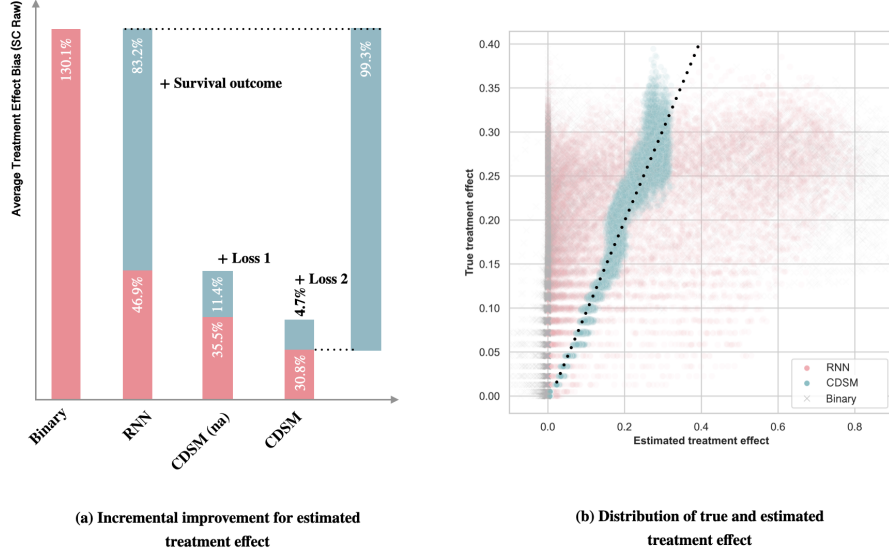
4.1 Experiments

In Table 2, we compare CDSM with the selected benchmarks (i.e., Binary, RNN and unadjusted CDSM), using the test data generated under the default simulated scenario. The Binary and RNN algorithms had better performance in estimating next-step survival (see AUROC and C-Index), while CDSM and its unadjusted version, CDSM(na) outperformed in the estimations of individual and average treatment effect measured by the differences in survival probabilities (SC (Raw)) and hazard ratios (HR (Raw)). The accuracy of CDSM is relatively consistent over time compared to the Binary and RNN models, as shown by the low standard deviation of the ATE bias over time (SC and HR (Raw Std)).

As expected, when the ATE is measured in terms of the difference in survival probabilities, the improvement from TMLE is negligible (Bias reduced from 30.8% to 29.9%) on CDSM since the treatment effect has already been adjusted. The correction is more noticeable for the Binary outcome model (130.1% to 40.5%) and the RNN (46.9% to 31.5%), where the raw estimation have high level of bias. On the other hand, adjustment using IPW made all raw estimations worse except for the Binary model. Similar observations have been found in ATE estimates measured by the hazard ratios.

CDSM gains most from its design of survival outcome and the potential outcomes sub-networks. In panel (a) of Figure 2, we assessed the incremental contribution to the reduction of ATE bias of each component of CDSM compared to the benchmarks by their raw ATE estimation defined in terms of the difference in survival probabilities, the RNN outperformed the Binary model by 83.2%. The inclusion of the sub-networks and concordance loss function

Figure 2: Diagnostic plots for CDSM



(a) Illustration of the incremental improvement from the design of CDSM on treatment effect estimations. The recorded absolute percentage bias (Bias) is averaged across 50 independent simulations over 30 time points from the test dataset under the default scenario. Abbreviations: survival outcome: changing binary outcome labels to survival outcome labels; Loss 1: concordance loss function and potential outcomes sub-networks; Loss 2: selection bias calibration loss function. (b) true and estimated individual treatment effect (ITE) distributions by benchmark algorithms. The colored dots are the true and estimated ITE at time 15 of a randomly chosen sample under the default scenario. The dashed diagonal line indicates the equation of the true and estimated values.

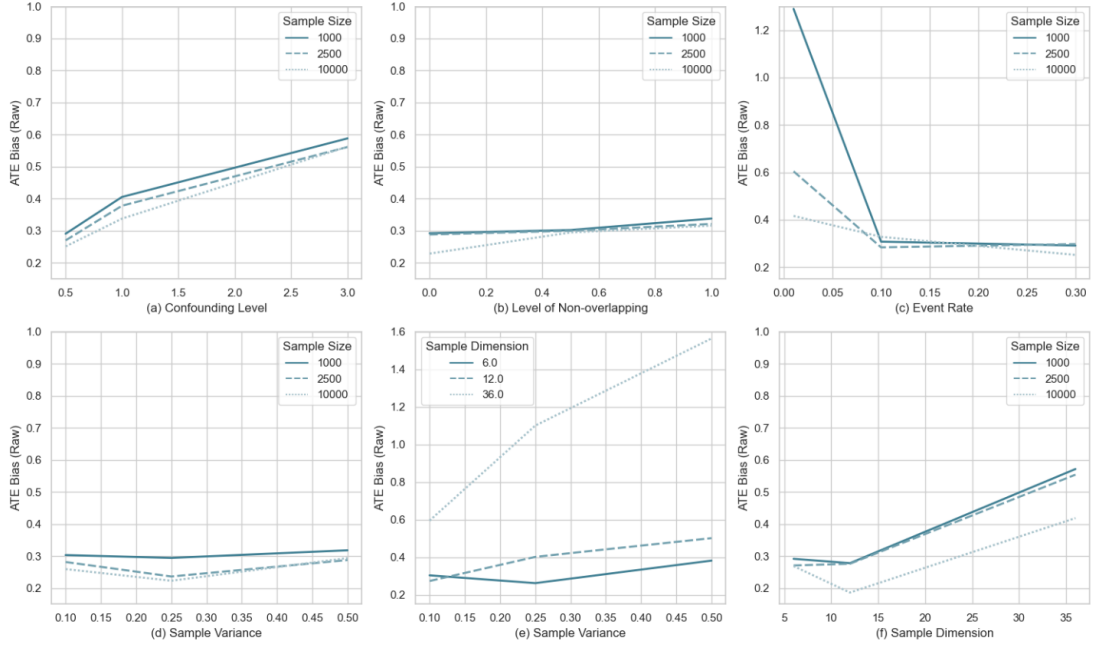
in CDSM (na) further reduced bias by 11.4%. Finally, the adjustment for selection bias improved estimation by another 4.7%.

Unlike the benchmark algorithms, CDSM provides ITE estimations closely following the true values. This is illustrated in panel (b) of Figure 2, which displays the true and estimated ITE distributions from a randomly chosen experiment under the default setting.

The performance of CDSM in ATE estimation was examined across different simulated scenarios in Figure 3. In general, larger sample sizes can improve the estimation accuracy for more complex data (i.e., higher level of dimension and sample variance; or lower level of overlapping and event rate). However, if the sample is strongly confounded, the improvement from larger sample is minimal (see panel (a) of Figure 3). The estimation accuracy is also sensitive to sample dimension. However, the correlation between sample dimension and variance is relatively small (see panel (e) of Figure 3) compared the sensitivity with the sample size. For high dimension EHR data, using a large sample with moderate level of overlapping could achieve better estimation accuracy.

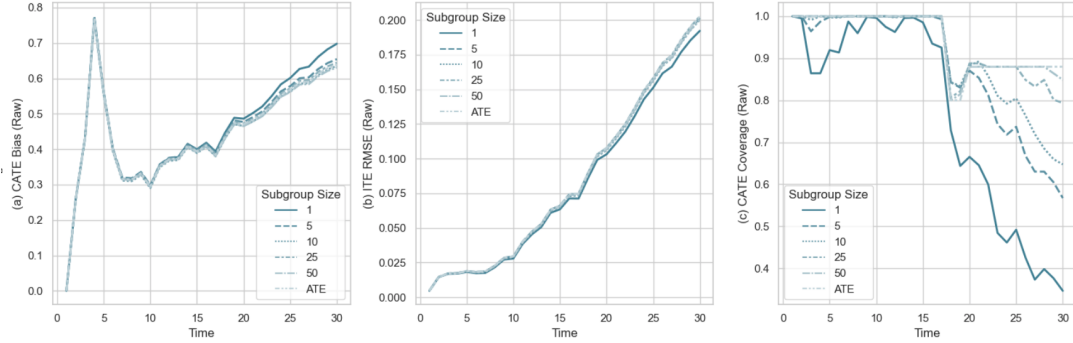
Lastly, we evaluate the estimations of CATE over time and subgroup sizes in panels (a) and (b) of Figure 4. The Bias and RMSE of the estimations increase with follow-up time. The initial jump in the Bias is caused by normalizing the Bias with the extreme small value of true treatment effect. The coverage ratio is displayed in panel (c). The model maintained a coverage ratio above 95% for the first 15 time steps but dropped sharply

Figure 3: Raw average treatment effect (ATE) estimation bias by scenarios



All metrics are averaged across 50 independent simulations over 30 time points from the test dataset under each scenario. Bias: average absolute percentage bias.

Figure 4: Raw conditional average treatment effect (CATE) estimation Bias, RMSE and the Coverage ratio by time and subgroup sizes.



Each subgroup is composed of M (subgroup size) randomly drawn individuals without replacement from a sample of size N . Each simulation is composed of N/M sub-samples of size M . All metrics are averaged across 50 independent simulations from the test dataset under the default scenario. Abbreviations: Bias: average absolute percentage bias; RMSE: Root-mean-square error; ITE: individual treatment effect.

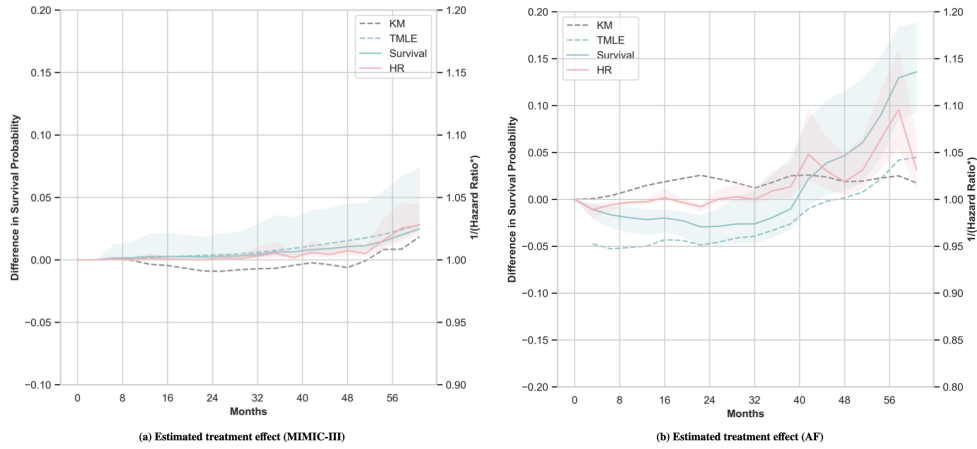
thereafter. In particular, the coverage for ITE estimations was reduced to around 40% at time 30, while for subgroups with group size greater than 25, the model still maintained the coverage above 80% by the end of simulation period. Given the similar level of Bias and

RMSE across subgroup sizes, panel (c) also tells us that CDSM provided more conservative quantile interval for larger subgroups.

4.2 Treatment effect estimation with clinical data

We applied CDSM to two clinical causal inference questions. MIMIC-III (Johnson et al., 2016) was used to study the effect of mechanical ventilation (MV) on the mortality of patients detected with sepsis. A different dataset, CPRD, was used to compare VKAs vs. NOAC in preventing three combined safety and efficacy outcomes in patients with non-valvular atrial fibrillation (AF).

Figure 5: Estimated treatment effect and hazard ratio* by benchmark algorithms.



The shaded area is the 95% quantile interval of the individual treatment effect estimations. Abbreviations: KM: Kaplan Meier estimator; TMLE: CDSM(na) estimation with TMLE adjustment; Survival: CDSM estimation; Hazard Ratio*: empirical hazard ratio.

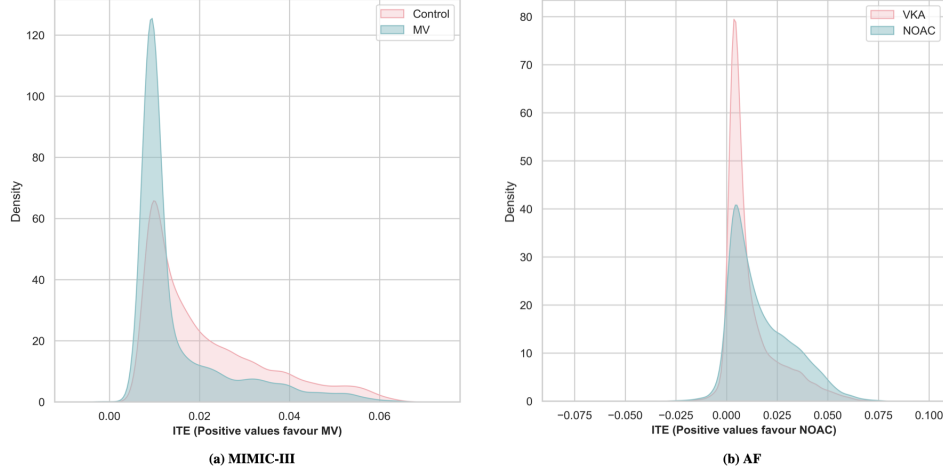
Figure 5 shows the estimations of ATE in terms of differences in survival probability using CDSM (labeled as Survival) and CDSM(na) with TMLE adjustment (labeled as TMLE). The absolute measure was also compared with the inversed empirical hazard ratio (i.e., $1/HR^*$, this is to make the hazard ratio has the same direction as the absolute difference) defined in Equation 7.

For MIMIC-III case study (panel (a)), the empirical hazard ratio ranges from 0.975 to 0.992, suggesting a minimal positive impact of using MV. The estimations indicate that the MV has its positive impact increases over time. By the 56th hour since the ICU admission, we can see the usage of MV is expected to reduce the probability of death by 2.24% (the 95% quantile interval of the ITE estimations is 1.26% to 7.23%) (Survival) or 3.04% (2.11%, 6.54%) (TMLE).

In the study of atrial fibrillation (panel (b)), the empirical hazard ratio over time ranged from 0.917 to 1.032. We observed an overall advantage of VKA over NOAC in the first 32 months and a salient benefit of NOAC over VKA thereafter. The estimated ATE suggests that using NOAC can improve the long term outcome of patients by reducing the probability of combined outcomes up to 13.83% (where the corresponding quantile interval is 9.11% to

17.25%) (for the detailed study on the long term benefits of using NOAC over VKA in atrial fibrillation patients, please refer to (Zhu and Gallego, 2021a)).

Figure 6: Distributions of estimated individual treatment effects (ITE) averaged over follow-up time



ITE estimations averaged over time in each study. Abbreviations: MV: mechanical ventilation; NOAC: Non-Vitamin K antagonist oral anticoagulants; VKA: Vitamin K antagonists.

Figure 6 depicts the distribution of estimated ITEs from CDSM averaged over time and colored by original treatment conditions. In the MIMIC-III dataset, we observed right skewed distributions of ITEs that favor the use of MV in both treatment groups. In the AF study, we identified small amount of patients have a negative ITE under both treatment conditions. Patients prescribed with VKA generally have minimal ITE from using NOAC.

5. Discussion

We have developed a novel casual inference algorithm using a causal deep Bayesian dynamic survival model, which we called CDSM. Our model estimates individual potential treatment response curves from sparse observational time series. It leverages information across individuals under different interventions with dedicated potential outcomes sub-networks. We demonstrated significant gains in accuracy of CDSM over plain recurrent neural networks in estimating individual and conditional average treatment effects.

In addition to extensive simulations, we applied CDSM on two observational clinical datasets, the MIMIC-III sepsis study and the CPRD atrial fibrillation study. Compared to the standard neural networks, we found CDSM has similar performance for the estimation of survival curves as DeepHit and Super-Learner models (the estimation performance of survival curves is presented in our working paper (Zhu and Gallego, 2021b)), but it is superior in identifying the treatment effect heterogeneity over time than existing methods. In particular, CDSM estimates the causal effect by computing the adjusted potential survival curves under treatment and control conditions. The use of propensity adjusted outcomes in the loss function helped to improve the estimation accuracy when the level of confounding

is high. In addition, CDSM learns from the pattern of missing covariates of a time series using masking layers rather than imputing their values, and it uses Bayesian dense layers to capture the epistemic uncertainty from the unknown underlying data generating process.

In this study, time-varying covariates have been simulated to resemble the observed data from a breast cancer clinical trial (Sauerbrei et al., 2000), where covariates followed a fractional polynomial function of time with two turning points. Since deep learning techniques do not assume specific functional dependences of treatments or outcomes, we expect our simulation results to hold under other choices of functional forms. Nevertheless, more extensive testing of CDSM under several simulation scenarios is desired and left for future work.

Our estimation quantile interval for ITEs is small and results in a low coverage ratio. This is owing to the model design where only one dense layer is initiated with Bayesian priors. The quantile interval will be more conservative if we allow more layer weights to be drawn from a prior. However, in this study, we are not answering the question of optimal choice of Bayesian layers, rather, our effort is to illustrate the potential to capture model uncertainty using a deep learning model.

One notable finding in this study is the strong effect of what we have called sample dimension on the treatment effect bias. However, it should be noted that in our simulations, all covariates represent informative confounders. We expect that, in real world high-dimensional datasets, most covariates are likely to represent noise or weak connections to treatment and outcome.

When comparing the ATE estimation from CDSM with that from traditional confounding-adjustment methods, we found our selection bias calibration loss function can achieve similar performance as TMLE but is much more accurate than IPW. The main drawback of IPW is that it applies the same weighting factor to the entire survival curve even though the covariates and outcome are time-varying.

In our case study, we do not explicitly use history previous to the beginning of follow-up, but rather patient history is contained in the baseline covariates such as the risk scores, which are estimated using the past 2 years of data. An alternative approach, which would improve the automation and reproducibility of the causal inference analysis, would be to include the full medical history as a time-series input. For example, rather than recording the prior history of intracranial hemorrhage (ICH) as a binary indicator (Lee et al., 2020b), we can input the timing of each occurrence of the ICH. The effect of this alternative strategy on the efficacy and performance of the model is left for future work.

The big challenge of longitudinal causal inference lays in its definition of treatment effect. In this study, treatment effect at a given time t has been defined as the difference in survival probability given treatment vs. control throughout the follow-up period $(t - u, t)$. However, when we have n treatments, we will face the choice of making the contrast among $n(n - 1)/2$ pairs. Nonetheless, the solution becomes more complicated when we consider the effect of a switch in treatment, that is, we need to consider the timing of the switch as well as the choice of effect contrast. Similarly, it is also arduous to analyze continuous treatments. Nonparametric methods have been proposed to either discretize the treatment options (Powell, 2020) or create splines to estimate the treatment effect on a single day (Kennedy et al., 2017). Few has been discussed for time-varying variables or treatments. One study (Komorowski et al., 2018) proposed to use reinforcement learning to control the

intravenous fluids dosage for sepsis patients, but it does not answer the question of causal effect nor does it adjust for potential confounding bias. It would be interesting for future studies to explore time-varying deconfounded treatment recommendations.

The proposed model as well as existing data-adaptive models are limited in their ability to capture the aleatoric uncertainty, which arises from the hidden variables or measurement errors, and cannot be reduced by collecting more data under the same experimental conditions. This is reflected in our scenario analysis where increasing the sample size cannot improve the estimation accuracy if the data is highly confounded. With observational data, the impact of confounding is often overlooked due to the limited ability to identify and collect potential confounders. A recent study (Wallach et al., 2020) found 74 out of 87 (85.1%) articles on the impact of alcohol on ischemic heart disease risk spuriously ignored or eventually dismissed confounding in their conclusions. Albeit this study acknowledges the caveats when interpreting results for the case studies, it will be important for future researches to quantify the aleatoric uncertainty for data-adaptive models.

CDSM fills the gap for causal inference using deep learning techniques for survival analysis. It considers time-varying and high-dimensional confounders with time-invariant treatment options. Its estimated absolute treatment effect can be easily compared with conventional literatures which use relative measures of treatment effect such as the hazard ratio. We expect CDSM will be particularly useful for identifying and quantifying treatment effect heterogeneity over time under the ever complex observational health care environment.

Acknowledgments

This work was supported by National Health and Medical Research Council, project grant no. 1125414. Ethics to use UK Clinical Practice Research Datalink data was obtained from ISAC (protocol number 17-093).

Appendix A. A. Average treatment effect estimation adjustment

A.1 Inverse probability weighting (IPW)

We apply the inverse probability weighting adjustment to the raw estimation of ATE with the following equation:

$$\hat{\psi}_{IPW}(t) = \frac{1}{N} \sum_{i=1}^n \left(\frac{A_i \hat{Y}_i(t)}{\hat{P}(X_i(0))} - \frac{(1 - A_i) \hat{Y}_i(t)}{1 - \hat{P}(X_i(0))} \right), \text{ where } t \in \{0, 1, \dots, \Theta\}$$

where N is the sample size, Θ is the maximum of follow-up time and $\hat{P}(X_i(0))$ is the propensity score estimated as the probability of receiving the treatment at time 0 if the treatment assignment is time-invariant. When the treatment is time-variant, we estimate the propensity score at each time step as $\hat{P}(X_i(t))$. In this study we estimated $\hat{P}(X_i(0))$ using a densely connected network to fit the binary label of the treatment assignment of each subject i at time 0.

A.2 The iterative targeted maximum likelihood estimation (TMLE)

To apply the iterative targeted maximum likelihood estimation adjustment, we conducted following adjustment at each time step:

1. We first calculate the smart covariates $H(A, X(t))$ using the propensity score estimated using the procedure aforementioned:

$$H(1, X_i(t)) = \frac{A_i}{\hat{P}(X_i(0))}; H(0, X_i(t)) = \frac{1 - A_i}{1 - \hat{P}(X_i(0))}$$

2. Then we fit the residual of the initial estimate of the logit of the binary label on smart covariates using an intercept-free regression:

$$\text{logit}(\hat{Y}_i(t)) - \text{logit}(Y_i(t)) = \delta_1(t)h(1, X_i(t)) + \delta_0(t)h(0, X_i(t))$$

where $\text{logit}(x)$ represents the function $\log(\frac{x}{1-x})$

3. Calculate the adjusted potential outcomes:

$$\hat{Y}_A(t)^1 = \log\left(\frac{\text{logit}(\hat{Y}_A(t) + \delta_A(t))}{P_A(X_i(0))}\right), \text{ for } A \in \{0, 1\}$$

where $\hat{P}_1(X_i(0)) = \hat{P}(X_i(0))$ and $\hat{P}_0(X_i(0)) = 1 - \hat{P}(X_i(0))$.

4. Targeted estimate of ATE at time t:

$$\hat{\psi}_{TMLE}(t) = \frac{1}{N} \sum_{i=1}^n (\hat{Y}_1(t)^1 - \hat{Y}_0(t)^1)$$

We illustrate the adjustment result on CDSM(na) in Figure 7

References

- Martín Abadi, Ashish Agarwal, Paul Barham, Eugene Brevdo, Zhifeng Chen, Craig Citro, Greg S. Corrado, Andy Davis, Jeffrey Dean, Matthieu Devin, Sanjay Ghemawat, Ian Goodfellow, Andrew Harp, Geoffrey Irving, Michael Isard, Yangqing Jia, Rafal Jozefowicz, Lukasz Kaiser, Manjunath Kudlur, Josh Levenberg, Dandelion Mané, Rajat Monga, Sherry Moore, Derek Murray, Chris Olah, Mike Schuster, Jonathon Shlens, Benoit Steiner, Ilya Sutskever, Kunal Talwar, Paul Tucker, Vincent Vanhoucke, Vijay Vasudevan, Fernanda Viégas, Oriol Vinyals, Pete Warden, Martin Wattenberg, Martin Wicke, Yuan Yu, Xiaoqiang Zheng, et al. TensorFlow: Large-Scale Machine Learning on Heterogeneous Systems, 2015.
- Susan Athey, Julie Tibshirani, and Stefan Wager. Generalized random forests. *The Annals of Statistics*, 47(2):1148–1178, 2019.
- Ioana Bica, Ahmed M Alaa, James Jordon, and Mihaela van der Schaar. Estimating counterfactual treatment outcomes over time through adversarially balanced representations. *arXiv preprint arXiv:2002.04083*, 2020.

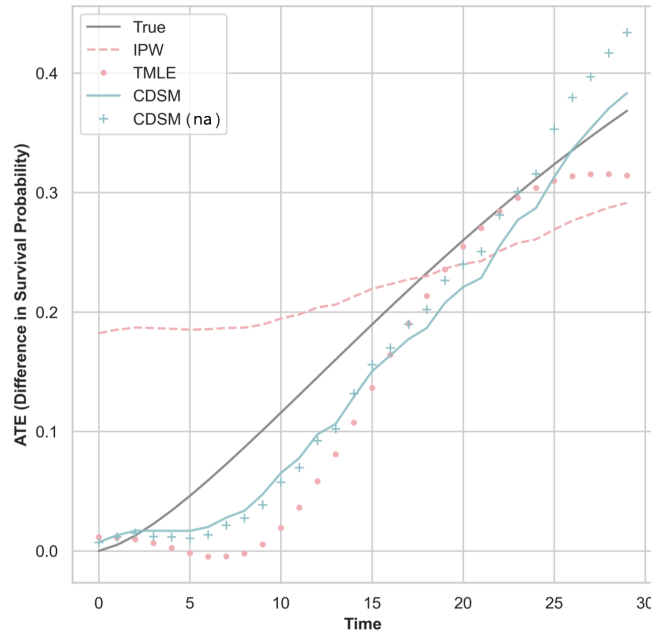


Figure 7: Estimated average treatment effect by benchmark algorithms. An illustration from a randomly selected experiment under the default settings.

John Blitzer, Ryan McDonald, and Fernando Pereira. Domain adaptation with structural correspondence learning. In *COLING/ACL 2006 - EMNLP 2006: 2006 Conference on Empirical Methods in Natural Language Processing, Proceedings of the Conference*, 2006. doi: 10.3115/1610075.1610094.

Zhengping Che, Sanjay Purushotham, Kyunghyun Cho, David Sontag, and Yan Liu. Recurrent Neural Networks for Multivariate Time Series with Missing Values. *Scientific Reports*, 8(1):1–12, 2018. doi: 10.1038/s41598-018-24271-9. URL <https://dx.doi.org/10.1038/s41598-018-24271-9>.

Victor Chernozhukov, Denis Chetverikov, Mert Demirer, Esther Duflo, Christian Hansen, Whitney Newey, and James Robins. Double/debiased machine learning for treatment and structural parameters. *Econometrics Journal*, 21(1):1–68, 2018. doi: 10.1111/ectj.12097.

Michael J Crowther and Paul C Lambert. Simulating biologically plausible complex survival data. *Statistics in medicine*, 32(23):4118–4134, 2013.

C R David. Regression models and life tables (with discussion). *Journal of the Royal Statistical Society*, 34(2):187–220, 1972.

E Frank, Robert M Harrell, David B Califf, Kerry L Pryor, Robert A Lee, and Rosati. Evaluating the yield of medical tests. *Journal of the American Medical Association*, 247(18):2543–2546, 1982.

- Blanca Gallego, Adam G Dunn, and Enrico Coiera. Role of electronic health records in comparative effectiveness research. *Journal of comparative effectiveness research*, 2(6): 529–532, 2013.
- Michael F. Gensheimer and Balasubramanian Narasimhan. A scalable discrete-time survival model for neural networks. *PeerJ*, 7:e6257–e6257, 2019. doi: 10.7717/peerj.6257. URL <https://dx.doi.org/10.7717/peerj.6257>.
- R. Henderson. Joint modelling of longitudinal measurements and event time data. *Biostatistics*, 2000. doi: 10.1093/biostatistics/1.4.465.
- Emily Herrett, Arlene M Gallagher, Krishnan Bhaskaran, Harriet Forbes, Rohini Mathur, Tjeerd van Staa, and Liam Smeeth. Data Resource Profile: Clinical Practice Research Datalink (CPRD). *International Journal of Epidemiology*, 44(3):827–836, 06 2015. doi: 10.1093/ije/dyv098.
- Sepp Hochreiter and Jürgen Schmidhuber. Long short-term memory. *Neural computation*, 9(8):1735–1780, 1997.
- Hans C. Van Houwelingen. Dynamic prediction by landmarking in event history analysis. *Scandinavian Journal of Statistics*, 2007. doi: 10.1111/j.1467-9469.2006.00529.x.
- Joseph G. Ibrahim, Haitao Chu, and Liddy M. Chen. Basic concepts and methods for joint models of longitudinal and survival data, 2010.
- Kosuke Imai and Aaron Strauss. Estimation of Heterogeneous Treatment Effects from Randomized Experiments, with Application to the Optimal Planning of the Get-Out-the-Vote Campaign. *Political Analysis*, 19(1):1–19, 2011. doi: 10.1093/pan/mpq035. URL <https://dx.doi.org/10.1093/pan/mpq035>.
- A Johnson, T Pollard, and L Shen. MIMIC-III, a freely accessible critical care database. *Sci Data*, 3:160035–160035, 2016.
- Alistair E. W. Johnson, Jerome Aboab, Jesse D. Raffa, Tom J. Pollard, Rodrigo O. Deliberato, Leo A. Celi, and David J. Stone. A Comparative Analysis of Sepsis Identification Methods in an Electronic Database*. *Critical Care Medicine*, 46(4):494–499, 2018. doi: 10.1097/ccm.0000000000002965. URL <https://dx.doi.org/10.1097/ccm.0000000000002965>.
- Edward H Kennedy, Zongming Ma, Matthew D McHugh, and Dylan S Small. Nonparametric methods for doubly robust estimation of continuous treatment effects. *Journal of the Royal Statistical Society. Series B, Statistical Methodology*, 79(4):1229, 2017.
- Matthieu Komorowski, Leo A. Celi, Omar Badawi, Anthony C. Gordon, and A. Aldo Faisal. The Artificial Intelligence Clinician learns optimal treatment strategies for sepsis in intensive care. *Nature Medicine*, 24(11):1716–1720, 2018. doi: 10.1038/s41591-018-0213-5. URL <https://dx.doi.org/10.1038/s41591-018-0213-5>.
- Richard L Kravitz, Naihua Duan, and Joel Braslow. Evidence-based medicine, heterogeneity of treatment effects, and the trouble with averages. *The Milbank Quarterly*, 82(4):661–687, 2004.

- Anand Kumar, Daniel Roberts, Kenneth E Wood, Bruce Light, Joseph E Parrillo, Satendra Sharma, Robert Suppes, Daniel Feinstein, Sergio Zanotti, and Leo Taiberg. Duration of hypotension before initiation of effective antimicrobial therapy is the critical determinant of survival in human septic shock. *Critical care medicine*, 34(6):1589–1596, 2006.
- Changhee Lee, Jinsung Yoon, and Mihaela van der Schaar. Dynamic-DeepHit: A Deep Learning Approach for Dynamic Survival Analysis With Competing Risks Based on Longitudinal Data. *IEEE Transactions on Biomedical Engineering*, 67(1):122–133, 2020a. doi: 10.1109/tbme.2019.2909027. URL <https://dx.doi.org/10.1109/tbme.2019.2909027>.
- So-Ryoung Lee, Eue-Keun Choi, Soonil Kwon, Jin-Hyung Jung, Kyung-Do Han, Myung-Jin Cha, Seil Oh, and Gregory YH Lip. Oral anticoagulation in asian patients with atrial fibrillation and a history of intracranial hemorrhage. *Stroke*, 51(2):416–423, 2020b.
- David Powell. Quantile treatment effects in the presence of covariates. *Review of Economics and Statistics*, 102(5):994–1005, 2020.
- Julie C. Recknor and Alan J. Gross. Fitting Survival Data to a Piecewise Linear Hazard Rate in the Presence of Covariates. *Biometrical Journal*, 1994. doi: 10.1002/bimj.4710360613.
- M Reyna, C Josef, R Jeter, S Shashikumar, B Moody, M B Westover, A Sharma, S Nemati, and G Clifford. Early Prediction of Sepsis from Clinical Data – the PhysioNet Computing in Cardiology Challenge, 2019. URL <https://doi.org/10.13026/v64v-d857>.
- S Rose and M J van der Laan. Targeted Learning: Causal Inference for Observational and Experimental Data. *Targeted Learning: Causal Inference for Observational and Experimental Data*, 2011. doi: 10.1007/978-1-4419-9782-1.
- Paul R. Rosenbaum and Donald B. Ruban. The central role of the propensity score in observational studies for causal effects. *Biometrika*, 70(1):41–55, 1983. doi: 10.1093/biomet/70.1.41. URL <https://dx.doi.org/10.1093/biomet/70.1.41>.
- W Sauerbrei, G Bastert, H Bojar, C Beyerle, RLA Neumann, C Schmoor, M Schumacher, et al. Randomized 2× 2 trial evaluating hormonal treatment and the duration of chemotherapy in node-positive breast cancer patients: an update based on 10 years’ follow-up. *Journal of clinical oncology*, 18(1):94–94, 2000.
- M. Schomaker, M. A. Luque-Fernandez, V. Leroy, and M. A. Davies. Using longitudinal targeted maximum likelihood estimation in complex settings with dynamic interventions. *Statistics in Medicine*, 2019. doi: 10.1002/sim.8340.
- C W Seymour. Assessment of clinical criteria for sepsis: For the third international consensus definitions for sepsis and septic shock (sepsis-3). *J. Am. Med. Assoc*, 315:762–774, 2016.
- Joshua D Wallach, Stylianos Serghiou, Lingzhi Chu, Alexander C Egilman, Vasilis Vasiliou, Joseph S Ross, and John PA Ioannidis. Evaluation of confounding in epidemiologic studies assessing alcohol consumption on the risk of ischemic heart disease. *BMC medical research methodology*, 20(1):1–10, 2020.

- Yeming Wen, Paul Vicol, Jimmy Ba, Dustin Tran, and Roger Grosse. Flipout: Efficient pseudo-independent weight perturbations on mini-batches. *arXiv preprint arXiv:1803.04386*, 2018.
- T Wendling, K Jung, A Callahan, A Schuler, N H Shah, and B Gallego. Comparing methods for estimation of heterogeneous treatment effects using observational data from health care databases. *Statistics in medicine*, 37(23):3309–3324, 2018.
- Jie Zhu and Blanca Gallego. Targeted Estimation of Heterogeneous Treatment Effect in Observational Survival Analysis. *Journal of Biomedical Informatics*, page 103474, jun 2020a. doi: 10.1016/j.jbi.2020.103474.
- Jie Zhu and Blanca Gallego. Targeted Estimation of Heterogeneous Treatment Effect in Observational Survival Analysis. *Journal of Biomedical Informatics*, page 103474, jun 2020b. doi: 10.1016/j.jbi.2020.103474.
- Jie Zhu and Blanca Gallego. Individualized estimates of the comparative effectiveness of noacs vs vkas in newly diagnosed non-valvular atrial fibrillation patients, 2021a.
- Jie Zhu and Blanca Gallego. Dynamic prediction of time to event with survival curves, 2021b.